1. Experimental set-up and measurements

The fire experiments consist of 2 Single Burning Item (SBI) tests [1], namely, an inert test with two Calcium Silicate (CS) panels, i.e., test CSCS [2], and a flame spread test with Medium Density Fiberboard (MDF) panels, i.e., test MM3 [3]. The experimental set-up of the SBI tests is presented here briefly, while more details are available in [2, 4].

As portrayed in Fig. 1, two test panels are placed in a vertical position and perpendicular to each other to form a corner. The *long panel* is 1.5 m high and 1.0 m wide, while the *short panel* is 1.5 m high and 0.5 m wide. The panels are conditioned prior to the tests at 21°C and 50% relative humidity. A triangular propane (C_3H_8) sandstone burner with side dimension of 0.25 m is located at a 0.04 m clearance from the panels. The main propane burner operates at 30 kW, representing a corner fire source at the bottom corner of the panels. When the main burner is ignited at the beginning of the experiments (t = 0 s), it takes less than 30 s for the burner to stabilize within ±1 kW of 30 kW (see Fig. 2).

The hood on top of the testing trolley extracts the gases at a flow rate of 0.6 Nm^3/s (i.e., normal cubic meter per second, obtained at 298 K), allowing to obtain the evolution profiles of total Heat Release Rate (HRR) and Smoke Production Rate (SPR) based on the concepts of oxygen depletion [5] and smoke obscuration [6], respectively. For the purpose of intial calibration, a period of 303 s seconds is considered before the actual test. During this intial period, the ambient oxygen and carbon dioxide concentrations are recorded for 120 s. Subsequently, an auxiliary (2nd) burner is switched on, located behind an inert screen further away from the panels (see Fig. 1). This secondary burner is identical to the main burner, with both the burners sharing the same propane supply line. In turn, this makes it possible to calibrate the propane flow rate for the desire burner HRR of 30 kW.

The flame spread is monitored using cameras from two different angles and measurements are made of the evolution of panel temperatures, total HRR and Smoke Production Rate (SPR), as well as the total heat fluxes at the standard thermal attack calibration points of SBI [1]. Moreover, the evolution of the panel temperatures is investigated via through-thickness temperature measurements at various locations over the burning panels. In addition, the evolution of temperatures at the backside of the burning panels is discussed.

Temperature measurements are made all over the panels at different depths and at the backside using K-type thermocouples, as depicted in Fig. 3. The through-thickness measurements are made by placing the thermocouples inside holes, drilled from the backside of the panels. Each thermocouple has its wires welded only at one terminal bead to ensure that through-thickness temperatures are recorded strictly at the desired depth. The thermocouple bead, sized approximately 0.0015 m, is fixed in place firmly using thermal

adhesive 940 HT-1 from Polytec PT in Germany. This paste provides superior thermal conductivity (with thermal conductivity of 2.1 W/(m.K), i.e. over 10 times that of the CS panels). Due to its alumina oxide base, the paste does not decompose at high temperatures and is electrically nonconductive so it does not interfere with the functioning of the thermocouples.

Measurements of total heat fluxes are made using water-cooled Schmidt-Boelter heat flux sensors with a working range up to 75 kW/m^2. As depicted in Fig. 3, the measurements are made at the three thermal attack calibration points set forth by Annex D.2 of SBI's standard [1]. As the combustion of propane from the burner yields a considerable amount of water vapor, condensation occurs on the cooled sensors, causing errors reported as high as 8% [7]. Therefore, as a conventional practice, the temperature of the cooling water supplied to the sensors is maintained at 50°C to diminish condensation errors. All the sensors are set flush with the surface of the panels.

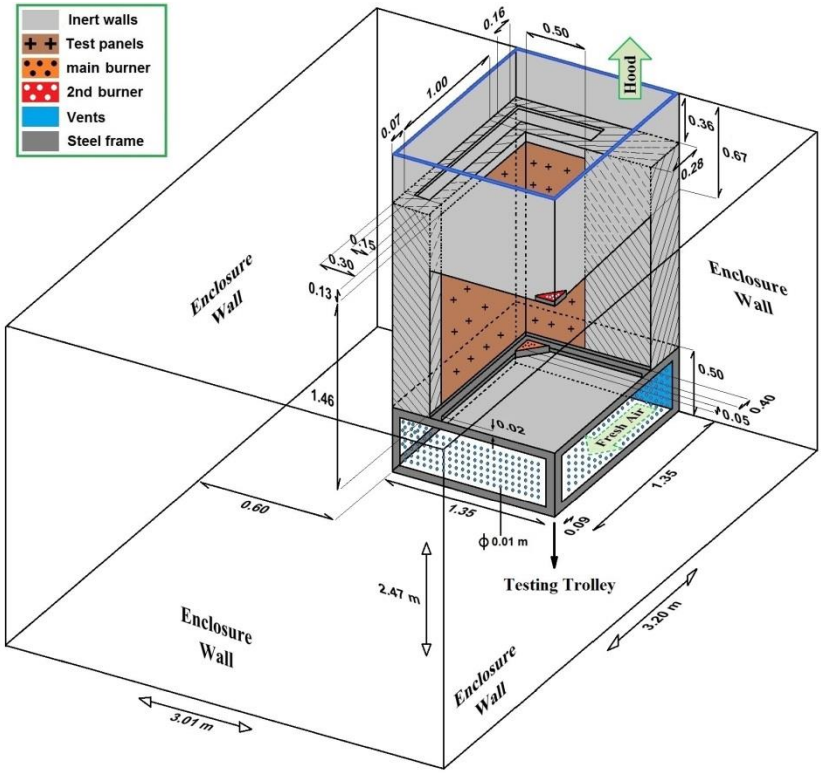

Fig. 1. SBI testing enclosure (units in m) [4]. There are two openings in the enclosure, namely, the hood on top of the testing trolley and the vent at the bottom of the backside of the trolley (1.16 m by 0.32 m) where fresh air enters the enclosure. To produce a more uniform airflow into the compartment, the bottom sides of the trolley are covered with perforated steel plates (0.01 m diameter perforations). The exposed height of the panels is 1.46 m, and there is an air gap behind each panel, i.e., 0.30 m wide behind the long panel and 0.28 m wide behind the short panel. The image is not to scale.

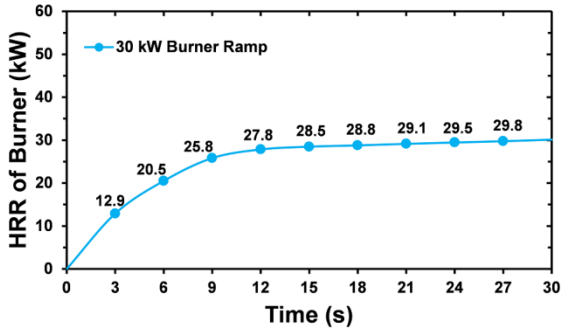

Fig. 2. The HRR ramp of the burner at the start of the SBI tests [2].

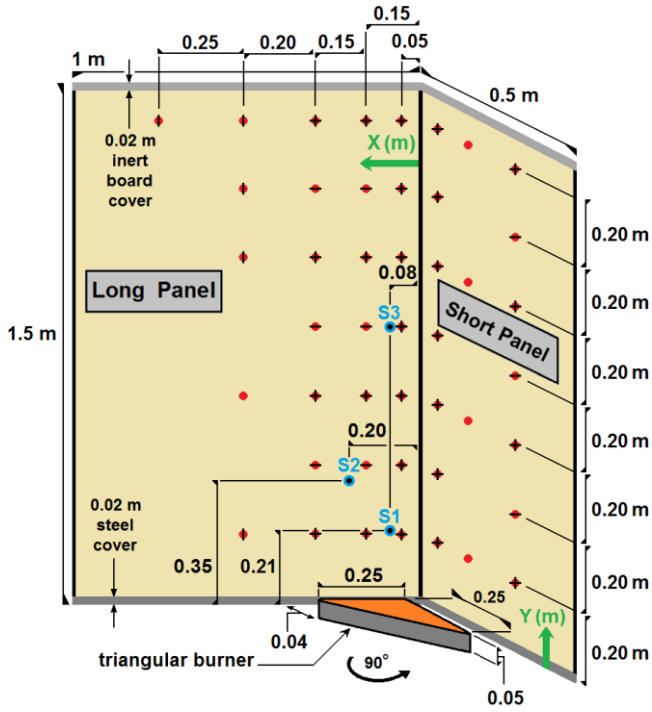

Fig. 3. The layout of the measurements on the panels in the SBI experiments (with distance units in meters) [4]. On the panels, temperatures are measured using thermocouples either only at the backside (●), at 0.001 m depth (from the front surface) and the backside (◐), at 0.002 m depth and the backside (⊖), or at 0.001 m, 0.002 m and the backside simultaneously (✚).Total heat fluxes are measured using sensors S1 to S3 (◉). Horizontal and vertical axes have been denoted with X and Y , respectively.

The pyrolysis front (defined as the outermost location at which the panel material has pyrolyzed and charred, as shown in Fig. 4) is visually tracked at multiple heights in the experimental footage. The time resolution of tracking is limited in the beginning of the test because fronts are initially covered by the burner flames. This does not affect the analysis of 'lateral flame spread'

starting after t = 180 s. Lateral flame spread is conventionally characterized in bench-scale tests using the LIFT apparatus [8], by exposing a long horizontal sample to a gas-fired radiant panel at an angle of 15°, with a non-impinging pilot flame at the hot end of the sample serving as the ignition source [9]. In the SBI tests, the flames above the burner serve as the corresponding pilot ignition source for lateral flame spread.

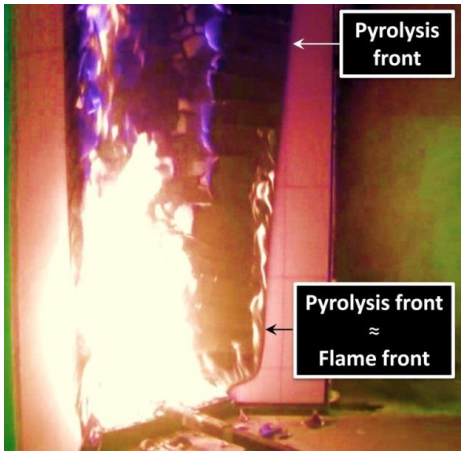

Fig. 4. Snapshot showing the pyrolysis front spreading laterally on the short panel in test MM3 [3]. The pyrolysis front is characterized by a dark boundary. In presence of flames, this follows the flame front [10].

2. Sample materials

Pictures of the sample panels and their example applications are shown in Fig. 5. The sample CS panels are 0.0123 m thick and their base material is calcium silicate, a light-weight powder that can be obtained by reacting calcium oxide (CaO) and silica (SiO_2) [11]. Due to its low thermal conductivity, calcium silicate is widely used for fireproofing and high temperature insulation as a safer alternative to asbestos. The material properties of the CS panels are presented in Table 1.

Table 1. Material properties of the sample CS panels [2]

Property	Value
Thickness [m]	0.0123 ± 0.001
Density [kg/m^3]	1005 ± 5%
Moisture content [%]	5 – 10
Thermal conductivity [W/(m.K)]	0.17[a]
Specific heat capacity [J/(kg.k)]	920[b]

[a] The nominal value of thermal conductivity is 0.17, 0.19 and 0.21 W/(m.K) at temperatures of 293, 373 and 473 K.

[b] The nominal value at 673 K.

Table 2. Material properties of the sample MDF panels [4]

Property	Value
Thickness [m]	0.0182 ± 0.003
Moisture content [%]	6–10
Effective thermal inertia [$kJ^2/(m^4.K^2.s)$]	0.906
Bulk density of virgin [kg/m^3]	585 ± 5%
Bulk density of char[a] [kg/m^3]	308 ± 10%
Net (lower) heating value of virgin [J/kg]	18.2×10^6
Net (lower) heating value of char[a] [J/kg]	23.4×10^6 ± 4%
Effective absorptivity of virgin [-]	$\alpha(T_{source})$ [b]
Effective emissivity of virgin [-]	$\varepsilon(T_{surf})$ [b]
Effective absorptivity and emissivity of char [-]	0.86[d]
Effective heat of combustion[c] [J/kg]	9.54×10^6
Time to ignition under 50 kW/m^2 [d] [s]	20–23
Effective critical heat flux [kW/m^2]	10
Char yield[d,e] [kg/kg]	0.14–0.18
Total average HRR[e,f] [kW/m^2]	90
300 s average HRR[e,f] (kW/m^2]	162
Average CO yield[e,f] [kg/kg]	0.03
Average CO_2 yield[e,f] [kg/kg]	0.98

[a] Based on the average of experiments in a cone calorimeter at incident heat fluxes of 15–75 kW/m^2.

[b] a and ε have been obtained using spectral measurements [12]. For the virgin material:

$$a(T_{source}) \text{ and } \varepsilon(T_{surf}) = 7.17\cdot10^{-21}T^6 - 7.90\cdot10^{-17}T^5 + 3.23\cdot10^{-13}T^4 ..$$
$$-5.65\cdot10^{-10}T^3 + 3.26\cdot10^{-7}T^2 - 1.28\cdot10^{-4}T + 9.34\cdot10^{-1}$$

where T_{source} and T_{surf} are the radiating source and panel surface temperatures, respectively.

[c] Based on an FPA test conducted at 50 kW/m^2 in normal atmosphere.

[d] Based on the average of 3 cone calorimeter experiments at 50 kW/m^2.

[e] Averaged from the ignition time until the burnout of the material.

[f] Average of the first 300 s.

The MDF panels are 0.018 m thick and their base material is softwood (no coarse fibers), with no isocyanates or phenol resins, bearing a first class rating for use in the European system [13]. This type of premium MDF panel meets low formaldehyde emission criteria of E1 category in Europe [14], i.e., as low as that of its natural wood source [15]. Thus, it is widely used for interior design and decoration, for example slotwalls, and generally for fixed furniture, such as cabinets. In addition to its customary applications, another reason for the selection of MDF in this study is the more isotropic nature of

this material compared to natural wood or other engineered wood products such as particle board (also known as chipboard). MDF does not contain knots or rings, and is manufactured through pressing of fine fibers of length typically below 0.001 m [16]. The resulting outer surface is hard, smooth and flat, while the inner core consists of soft fibers with lower density [17]. The measured material properties of the sample MDF panels are presented in Tables 2 and 3.

Fig. 5. Sample CS and MDF panels (top and bottom, respectively) along with pictures of their example applications [18, 19].

Table 3. Ignition time at different heat fluxes for the sample MDF panels [4]

Incident heat flux (kW/m^2)	**Time of ignition, t_{ig} (s)**	
	Experiment 1	Experiment 2
15	224	219
25	100	98
50	29	22
75	13	10

3. Data of the SBI tests

3.1. Footage

CSCS footage (long panel): https://drive.google.com/open?id=0B--yr0puiIShMFI2WGJ0R05HTWM
MM3 footage (long panel): https://drive.google.com/open?id=0B--yr0puiIShWG9kNDNoU2gzNXM
MM3 footage (short panel): https://drive.google.com/open?id=0B--yr0puiIShb1J1U0plc1o5MjQ

3.2. Total HRR and SPR

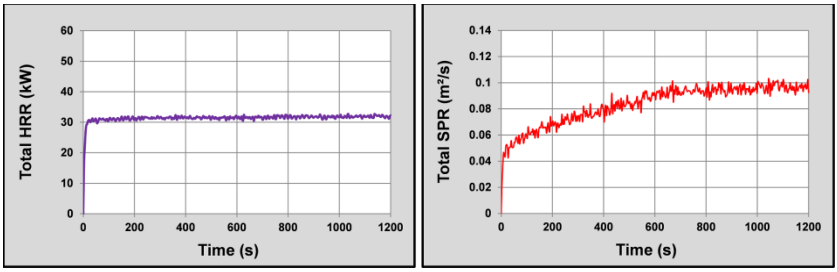

Fig. 6. Total HRR (left) and total SPR (right) in test CSCS.
Data file: https://drive.google.com/open?id=1ZxpuxXUN--lVbLWQygyUzWJ9hroatFOU

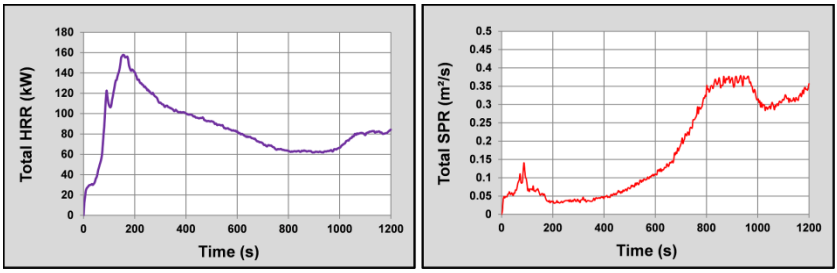

Fig. 7. Total HRR (left) and total SPR (right) in test MM3.
Data file: https://drive.google.com/open?id=1hpD_xeUoAlfg63trApy3foS4AOwcUbte

3.3. Total heat fluxes

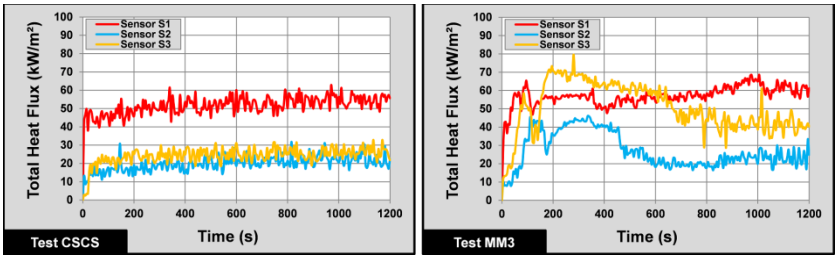

Fig. 8. Total heat fluxes in tests CSCS and MM3. See Fig. 3 for the sensor positions.
Data of CSCS: https://drive.google.com/open?id=1iaZXCYplROpsYudTaVwC67YOK-7TV8cy
Data of MM3: https://drive.google.com/open?id=13-gAK8oWZdWZN0-nIgPHxTAk-pOHCGbU

3.4. Flame heights

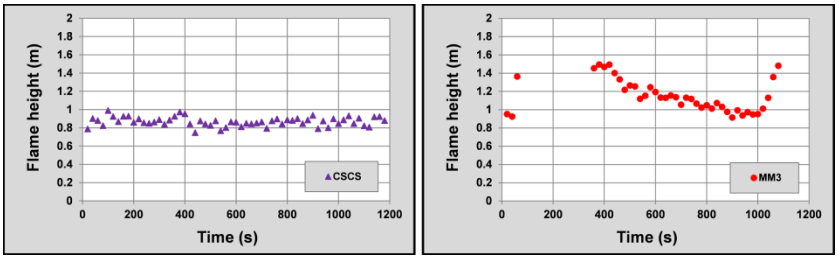

Fig. 9. Evolution of instantaneous flame heights, averaged over 2 s windows, in test CSCS (left) versus those in test MM3 (right). The footage height limit is 1.7 m so average values higher than 1.5 m are not considered to avoid introduction of clipped data [3].

Data of CSCS: https://drive.google.com/open?id=1-MEfp-abfVLUqc0_SCOrKU9Co30bcK7I
Data of MM3: https://drive.google.com/open?id=1UCddyFfnGOsk2r2UoDwRV4qNsGPtBwTA

3.5. Panel temperatures

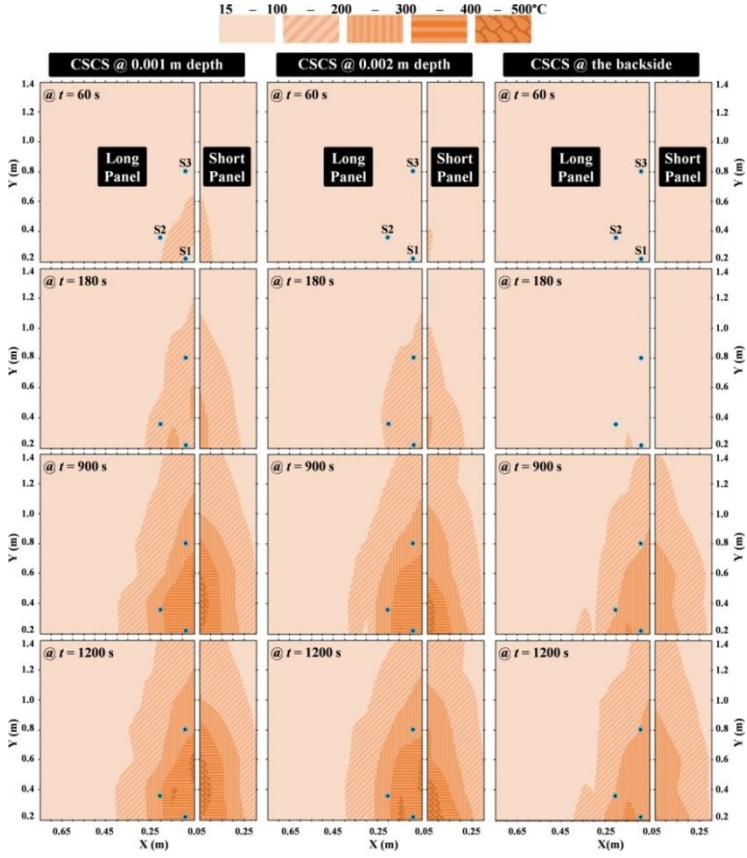

Fig. 10. The evolution of the panel temperatures in test CSCS [2].
Source data: https://drive.google.com/open?id=1-12DrnMsUPGZsElSUemGa7neqLXOOgmv

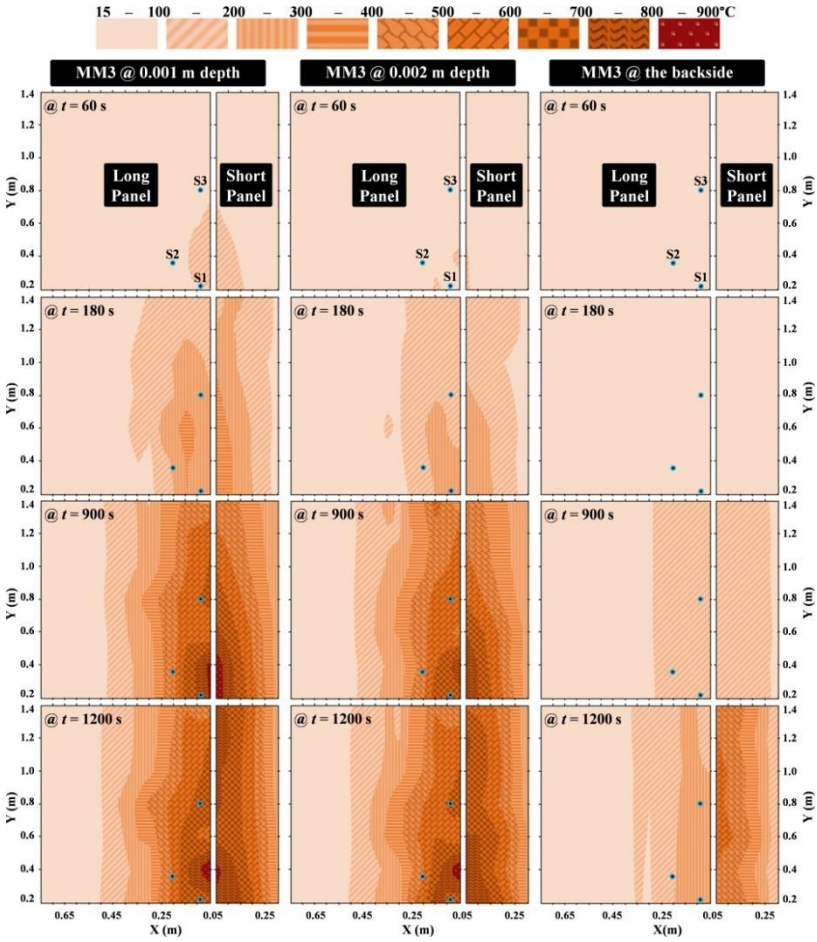

Fig. 11. The evolution of the panel temperatures in test MM3 [3].

Source data: https://drive.google.com/open?id=1-w1HSFXdm2xSqPwgxe6bVf6BAyeMpeh-

3.6. Pyrolysis front propagation

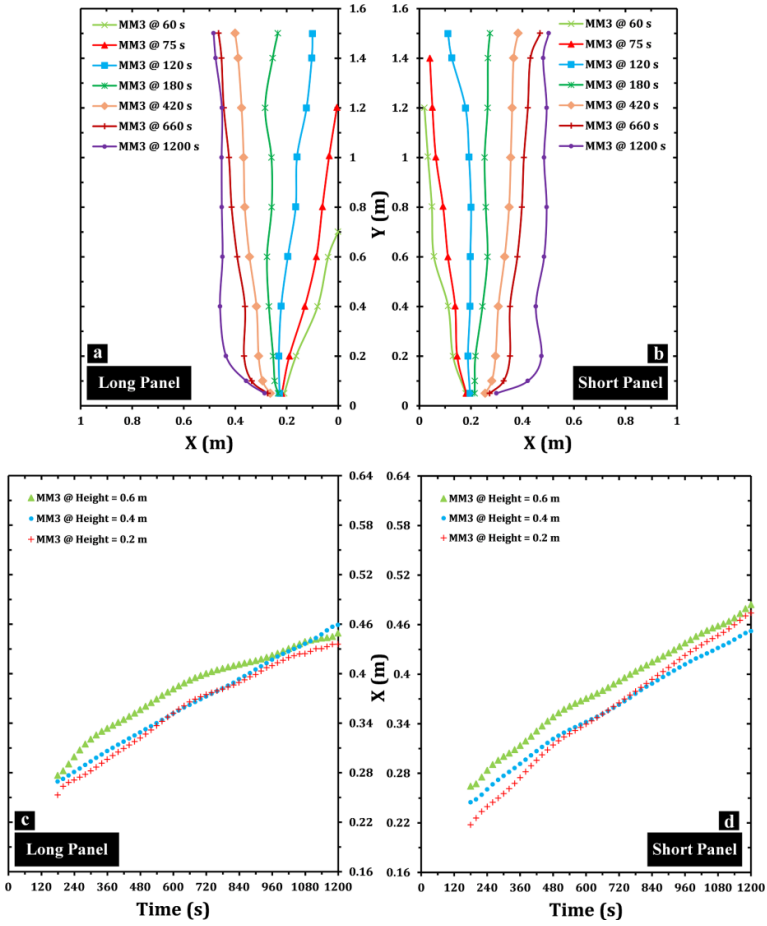

Fig. 12. Pyrolysis front propagation on the long and short panels in test MM3 [3]. X and Y denote the horizontal and vertical distances of the spread front from the corner, respectively. The definition of pyrolysis front is given in Fig. 4.

Data of long panel: https://drive.google.com/open?id=1QSU4mYN-f9Mp2qh5R5c-NIjrTFSBca2N
Data of short panel: https://drive.google.com/open?id=1yoU2QbbMjzlRdTcIcWgIwRFPFgqK9XZM

Bibliography

[1] EN-13823, "Reaction to fire tests for building products - Building products excluding floorings exposed to the thermal attack by a single burning item," European Standard, 2014.

[2] D. Zeinali, S. Verstockt, T. Beji, G. Maragkos, J. Degroote, and B. Merci, "Experimental study of corner fires—Part I: Inert panel tests," *Combustion and Flame,* vol. 189, pp. 472–490, 2018.

[3] D. Zeinali, S. Verstockt, T. Beji, G. Maragkos, J. Degroote, and B. Merci, "Experimental study of corner fires—Part II: Flame spread

over MDF panels," *Combustion and Flame,* vol. 189, pp. 491–505, 2018.
[4] D. Zeinali, "Flame Spread and Fire Behavior in a Corner Configuration," Doctoral Thesis, Department of Structural Engineering, Ghent University, Gent, Belgium, 2019.
[5] M.L. Janssens, "Measuring rate of heat release by oxygen consumption," *Fire Technology,* vol. 27, pp. 234-249, 1991.
[6] B.A.-L. Östman, "Smoke and Soot," in *Heat Release in Fires*, V. Babrauskas and S. J. Grayson, Eds., ed: Taylor & Francis, 1990, pp. 233-250.
[7] B.T. Lee, "Standard room fire test development at the National Bureau of Standards," presented at the Fire safety: Science and Engineering, Philadelphia, PA, 1985.
[8] ASTM-E1321-13, "Standard Test Method for Determining Material Ignition and Flame Spread Properties." West Conshohocken, Pennsylvania, US: ASTM International, 2013.
[9] D. Zeinali, D. Koalitis, and J. Schmid, "Guide for Obtaining Data from Reaction to Fire Tests." Switzerland: ETH Zürich, 2018.
[10] B.Y. Lattimer and U. Sorathia, "Thermal characteristics of fires in a combustible corner," *Fire Safety Journal,* vol. 38, pp. 747-770, 2003.
[11] H.F.W. Taylor, *Cement Chemistry*: Thomas Telford, 1997.
[12] G. Agarwal, M. Chaos, Y. Wang, D. Zeinali, and B. Merci, "Pyrolysis Model Properties of Engineered Wood Products and Validation Using Transient Heating Scenarios," presented at the 14th International Conference and Exhibition on Fire Science and Engineering, Royal Holloway College, Nr Windsor, UK, 2016.
[13] EN-335, "Durability of wood and wood-based products. Use classes: definitions, application to solid wood and wood-based products," European Standard, 2013.
[14] EN-ISO-12460-5, "Wood-based panels – Determination of formaldehyde release – Extraction method (called the perforator method)," European Standard, 2015.
[15] M. Bohm, M.Z. Salem, and J. Srba, "Formaldehyde emission monitoring from a variety of solid wood, plywood, blockboard and flooring products manufactured for building and furnishing materials," *J Hazard Mater,* vol. 221-222, pp. 68-79, 2012.
[16] B. Park;, Y. Kim;, and B. Riedl;, "Effect of Wood-Fiber Characteristics on Medium Density Fiberboard (MDF) Performance," *Journal of the Korean Wood Science and Technology,* vol. 29, pp. 27–35, 2001.
[17] X. Wang, M. Mohammad, L.J. Hu, and A. Salenikovich, "Evaluation of density distribution in wood-based panels using X-ray scanning," in *Proceedings of the 14th International Symposium on Nondestructive Testing of Wood*, University of Applied Sciences Eberswalde, Germany, 2005.
[18] Jiangyin-Shangpin-Chemical-Co.-Ltd. (Jan 28, 2019). *Caclium silicate board ceiling application*. Available: http://www.puglue.com/uploads/allimg/170323/1-1F323114915426.jpg
[19] Action-TESA. (Jan 28, 2019). *Prelaminated MDF and HDF Board Application*. Available: http://www.actiontesa.com/images/Action-TESA-Prelaminated-MDF-and-HDF-Board-Application-1.jpg